doi:10.1093/brain/awq218 Brain 2010: 133; 2942–2951 | 2942

BRAIN
A JOURNAL OF NEUROLOGY

Opa1 deficiency in a mouse model of dominant optic atrophy leads to retinal ganglion cell dendropathy

Pete A. Williams,[1] James E. Morgan[1,2] and Marcela Votruba[1,2]

1 School of Optometry and Vision Sciences, Cardiff University, Cardiff CF24 4LU, UK
2 Cardiff Eye Unit, University Hospital of Wales, Cardiff C14 4XW, UK

Correspondence to: Dr Marcela Votruba, MD, PhD,
FRCOphth, School of Optometry Vision Sciences,
Maindy Road,
Cardiff University,
Cardiff CF24 4LU, UK
E-mail: votrubam@cardiff.ac.uk

The heterozygous mutation B6;C3-*Opa1*^{Q285STOP}, which models autosomal dominant optic atrophy, leads to a 50% reduction in Opa1 transcript and protein in the mouse retina and neural tissues and is associated with visual dysfunction and structural changes in the murine retina and optic nerve. In this article we use this model to quantify and evaluate the dendritic morphology of retinal ganglion cells. Retinal ganglion cells in Opa1$^{+/-}$ mutant mice ($n = 16$) and accompanying age- and sex-matched controls ($n = 11$) (age ranges of <10, 10–15 and >20 months) were labelled DiOlistically with carbocyanine dyes to quantify changes in dendritic tree architecture as a function of age. We observed localized dendritic reduction to sublamina *b* of the inner plexiform layer without retinal ganglion cell loss, showing dendritic pruning of on- but not off-centre retinal ganglion cells, and this effect was exacerbated with age. The mean dendritic field area was reduced in on-centre retinal ganglion cells of 10- to 15-month-old mice (−24.24%; $C_V = 0.68$; $P < 0.05$) and >20-month-old mice (−43.22%; $C_V = 0.75$; $P < 0.05$) compared with age-matched wild-type controls. Similar changes were seen in average total dendritic length in on-centre retinal ganglion cells of 10- to 15-month-old mice (−31.66%; $C_V = 0.67$; $P < 0.05$) and >20-month-old mice (−49.55%; $C_V = 0.63$; $P < 0.05$). Sholl analysis showed a marked difference in the dendritic arborization of on-centre retinal ganglion cells in the 10- to 15-month-old group (area under the curve −21.67%; $P > 0.05$) and of the >20-month-old group (area under the curve −42.12%; $P < 0.05$) compared with the control group. There was no detectable change in dendritic morphology in <10-month-old Opa1$^{+/-}$ mutant mice compared with wild-type ($P > 0.05$). No significant changes ($P > 0.05$) were seen in off-centre retinal ganglion cells. Finally, there was also no significant change ($P > 0.05$) in the retinal ganglion cell count across all age groups. In conclusion, we show dendritic pruning in on-centre retinal ganglion cells of the Opa1$^{+/-}$ mouse model of autosomal dominant optic atrophy from as early as 10 months of age. These results highlight the importance of normal mitochondrial fusion balance, as influenced by the OPA1 protein in maintaining the dendritic morphology of retinal ganglion cells. Dendritic pruning precedes the onset of clinical visual loss and structural changes in the optic nerve in the absence of significant cell loss.

Keywords: Opa1; retinal ganglion cells; dendrite; dominant optic atrophy; mitochondria

Abbreviations: AUC = area under the curve; RGC = retinal ganglion cell

Received April 15, 2010. Revised May 27, 2010. Accepted June 26, 2010. Advance Access publication September 3, 2010

Introduction

Following the identification of *OPA1* as the gene mutated in many patients with autosomal dominant optic atrophy (Alexander *et al.*, 2000; Delettre *et al.*, 2000), detection of mutations in the *OPA1* gene (Ferre *et al.*, 2005) has provided valuable insights into the relationship between mitochondrial structure and neuronal viability. Autosomal dominant optic atrophy is the most common inherited optic neuropathy (prevalence 1:12 000) (Carelli *et al.*, 2002, 2007). The clinical features are a bilateral, symmetrical and painless loss of visual acuity, colour vision defects, central visual field loss and atrophy of the optic disc (Votruba *et al.*, 1998). The optic neuropathy is slowly progressive and is currently irreversible and untreatable. Over 200 mutations in *OPA1* have been identified so far in patients with autosomal dominant optic atrophy (http://lbbma.univ-angers.fr). How the 'dysfunction' of *OPA1*, which is ubiquitously expressed (Aijaz *et al.*, 2004), results in autosomal dominant optic atrophy remains unknown. The observation that homozygous $Opa1^{-/-}$ mice die after the embryonic stage E8.5 (Alavi *et al.*, 2007; Davies *et al.*, 2007) indicates that Opa1 function is essential. *OPA1* is present in the cells of the retinal ganglion cell (RGC) layer, inner and outer plexiform layers, and the inner nuclear layer (Aijaz *et al.*, 2004).

Opa1 has multiple functions: it participates in mitochondrial dynamics (inner membrane fusion) and together with mitofusins (Mfn1 and Mfn2) regulates mitochondrial network and morphology (Chen *et al.*, 2005). It is involved in the organization of cristae, oxidative phosphorylation maintenance and membrane potential maintenance, and in the control of apoptosis by the compartmentalization of cytochrome *c*.

The integrity of the mitochondrial network is essential for the maintenance of neuronal structure and function (Li *et al.*, 2004). In neurons with high metabolic demands, mutations in genes that are critical for mitochondrial function result in marked neuronal loss in a range of neurodegenerative diseases, The key known mitochondrial shaping proteins, comprising mitofusins Mfn1 and Mfn2, Opa1, Fis1 and Drp1, control normal fusion and fission in mitochondria (Chen *et al.*, 2003). Of these mutations in *OPA1*, *Mfn1 and Drp1* have so far been linked with human diseases: autosomal dominant optic atrophy (Alexander *et al.*, 2000; Delettre *et al.*, 2000), Charcot–Marie–Tooth Disease 2A (Palau *et al.*, 2009) and encephalopathy, optic atrophy and lactic acidosis (Waterham *et al.*, 2007), respectively. The role of mitochondria in ageing neural tissue is increasingly being recognized in diseases such as Alzheimer's, Parkinson's and Huntington's diseases. In these diseases, neural loss is gradual and is preceded by prolonged periods of neuronal compromise (Tatsuta and Langer, 2008). The high energy dependence of neurons renders them particularly susceptible to changes in mitochondrial function (Chen *et al.*, 2007; Twig *et al.*, 2008). They rely heavily on this for the maintenance of key neuronal functions such as the maintenance of membrane potentials, channel activity, saltatory conduction and synaptic transmission. The appropriate distribution of mitochondria in axons, at synapses and in dendrites is critical for synaptic plasticity and function.

Since mitochondria are critical for the establishment of neuronal connectivity and the maintenance of synaptic contacts (Li *et al.*, 2004), we reasoned that the effects of *OPA1* mutations would, at least in the early stages, manifest more as changes in neuronal connectivity and the maintenance of dendritic tree architecture. We hypothesize that these changes occur prior to the onset of significant RGC loss. We therefore studied changes in dendritic tree architecture in Opa1 mutant mice, over time, correlating these with changes in the RGC population and RGC function. Here we provide, for the first time, evidence that *OPA1* mutation leads to RGC dendritic pruning and morphological changes in the absence of widespread RGC loss.

Material and methods

Retinal preparation

Adult $Opa1^{+/-}$ experimental mice ($Opa1^{+/-}$) ($n = 21$) and their littermate controls ($n = 16$) were analysed as three age groups: <10, 10–15 and >20 months old. Exact wild-type mice ages were 4 ($n = 2$), 7 ($n = 2$), 10 ($n = 4$), 15 ($n = 1$), 20 ($n = 2$) and 24 ($n = 5$) months old and exact $Opa1^{+/-}$ mice ages were 4 ($n = 2$), 7 ($n = 2$), 10 ($n = 4$), 15 ($n = 1$), 20 ($n = 2$), 21 ($n = 2$), 23 ($n = 3$) and 24 ($n = 5$) months old. Mice were killed by cervical dislocation and the eyes quickly enucleated and placed in chilled (4°C) Hanks' balanced salt solution (Invitrogen, UK). The eye was punctured at the limbus and a slit cut in sclera to remove the cornea and sclera anterior to the ora serrata, lens and vitreous. Three cuts were made in the retina before being flat-mounted, ganglion cell layer up, on a cell culture insert (Millipore, Billerica, MA, USA) and submerged in custom media containing Neurobasal media, 2% B-2 supplement, 1% N-27 supplement and 0.5 mM glutamate (Invitrogen, UK). Retinas were incubated at 37°C and 4% CO_2 ready for DiOlistic labelling using a gene gun or labelling with Hoechst 33258 stain. The total time between death and DiOlistic labelling was <10 min.

DiOlistic labelling using the gene gun

The setting for the bead delivery and preparation has been described in detail earlier (Gan *et al.*, 2000; Sun *et al.*, 2002; Pignatelli *et al.*, 2004). In brief, 100 mg tungsten particles (1.7 μm; Bio-Rad, Hercules, CA, USA) were placed in a thin, even layer on a clean glass slide. About 80 mg of 1,1′-dioleyl-3,3,3′,3′-tetramethylindocarbocyanine methanesulphonate (Invitrogen) or 3,3′-dihexadecyloxacarbocyanine perchlorate (Invitrogen) was then suspended in 800 μl of methylene chloride, mixed and applied over the tungsten particles. The methylene chloride evaporated quickly to leave 1,1′-dioleyl-3,3,3′,3′-tetramethylindocarbocyanine methanesulphonate- or 3,3′-dihexadecyloxacarbocyanine perchlorate-coated tungsten particles, which were then scraped off using a surgical blade onto clean wax-paper or tinfoil. This powder was then funnelled into a length of tubing (Bio-Rad) and allowed to settle, resulting in a light application of the powder upon the inside of the tubing. Excess powder was funnelled off and the tubing was cut into 1.2 cm lengths, using a surgical blade, for storage in the dark at room temperature, ready for use.

Retinas were shot once at 100 psi using a Helios gene gun (Bio-Rad) from 5 cm with a 3.0 μm pore size, high pore density, cell culture insert (Becton Dickinson, Franklin Lakes, NJ, USA) to block clumps of

tungsten particles that were not properly separated. Retinas were then incubated for 25 min to facilitate dye diffusion before being placed in 4% paraformaldehyde for a further 35 min for light fixation. Retinal preparations were then mounted on a slide with ProLong Gold AntiFade Reagent (Invitrogen) and sealed with nail polish. Six retinas were further mounted with a 1 μg/ml Hoechst 33258 stain for RGC counts.

RGC dendritic morphological analysis

Image stacks of 145 on-centre and 21 off-centre RGCs were collected using a Zeiss LSM 510 confocal microscope (Carl Zeiss Ltd, UK) captured at a 20× objective allowing the whole dendritic field to be shown. Cells were pseudo-coloured cyan using a custom look-up table for better contrast. Specific dendritic morphologies were analysed using ImageJ to measure dendritic field area (measured using the convex polygon tool to join the outer most points of the dendritic tree), an ImageJ plugin, NeuronJ to measure total dendritic length, and a custom MATLAB macro to run a Sholl analysis (Sholl, 1953; Gutierrez, 2007). Statistics were performed using the Statistical Package for the Social Sciences (SPSS, Chicago, IL, USA) and Microsoft Excel (Microsoft, Redmond, WA, USA).

RGC counts

Six retinas were stained with Hoechst 33258 stain to allow for RGC cell counts. Images were taken from the RGC layer at three locations of the retina, 1 mm from the optic disc (directly dorsal to the centre of the optic disc, at 120° to this; ventral-nasally, and at 120° to this again; ventral-temporally) using a Leica DM6000 B confocal microscope (Leica Microsystems, UK) with a 20× objective. Cells were manually counted in a 250 μm^2 area using the ImageJ counter plugin. A further 10 retinal cross sections of wild-type ($n=5$) and *Opa1*$^{+/-}$ mice ($n=5$) were mounted with Haematoxylin and Eosin. These sections were collected from five areas that were 20 sections apart. Images of the whole retina were obtained using a Leica DMRA2 microscope equipped with a camera DC500 (Leica) and QWinV3 software, and the RGCs manually counted. These data were combined and then expressed as a percentage change between wild type and *Opa1*$^{+/-}$ mice.

Results

Opa1 deficiency leads to RGC dendropathy, which is exacerbated with age and is localized exclusively to sublamina *b* (on-centre layer) of the inner plexiform layer

One hundred and forty five RGCs were identified as on-centre, based on their ramification within the inner plexiform layer and their dendritic field areas, total dendritic lengths and dendritic complexities, measured as outlined in the 'Material and methods' section. A panel of on-centre RGCs across all age groups can be seen in Fig. 1. All cells were confirmed to be RGCs by the presence of axons running in the retinal nerve fibre layer towards the optic disc.

Dendritic structure shows age-related degeneration in *Opa1*$^{+/-}$

Our results show a significant decrease in the average total dendritic area of *Opa1*$^{+/-}$ on-centre RGCs in both the 10- to 15-month-old group (−24.24%; $C_V=0.68$; $P=0.054$) (Student's *t*-test) and the >20-month-old group (−43.22%; $C_V=0.75$; $P=0.025$), but not in the <10-month-old group (−9.24%, $C_V=0.58$, $P=0.584$) (Fig. 2A). Similar changes were also seen with measurements of total dendritic length of *Opa1*$^{+/-}$ on-centre RGCs in both the 10- to 15-month-old group (−31.66%; $C_V=0.67$; $P=0.008$) and the >20-month-old group (−49.55%; $C_V=0.63$; $P=0.021$) but not the <10-month-old group (−0.30%; $C_V=0.49$; $P=0.984$) (Figs 2B and 3).

Dendritic complexity

Dendritic complexities were also analysed using a custom MATLAB macro to run a Sholl analysis where dendrites are measured when they intersect graded concentric circles of 10 μm around the soma (see Gutierrez, 2007). Sholl analyses were run using a ring interval of 10 μm. Our results show a decrease in the dendritic complexities of on-centre RGCs in both the *Opa1*$^{+/-}$ 10- to 15-month-old group [area under the curve (AUC) –21.67%; $P>0.05$] and >20-month-old group (AUC –42.12%; $P<0.05$) but not in the <10-month-old group (AUC –1.29%; $P>0.05$) (Fig. 4).

Opa1 deficiency has no effect on RGC count

Cell counts were derived from either Hoechst stained flat-mounts or Haematoxylin and Eosin stained sections from both wild-type (<10-month-old, $n=1$; 10- to 15-month-old, $n=2$; >20-month-old, $n=5$) and *Opa1*$^{+/-}$ mice (<10-month-old, $n=1$; 10- to 15-month-old, $n=2$; >20-month-old, $n=5$) (Fig. 5). Results show no significant change ($P>0.05$) in RGC count across all age groups, suggesting no RGC loss. Previous findings by our group in the same animal model show no change in the number of axons per area optic nerve between wild-type and *Opa1*$^{+/-}$ at 6, 9 and 24 months of age (White *et al.*, 2009), again suggesting no RGC death.

Opa1 deficiency has no effect on off-centre RGCs in all age groups

A further 21 RGCs were identified as off-centre based on their ramification within the inner plexiform layer (Xu *et al.*, 2007). There was no significant change in the dendritic morphologies of *Opa1*$^{+/-}$ off-centre RGCs even in the >20-month-old group (Fig. 6). Off-centre RGCs appear to have an unchanged ($P>0.05$) dendritic field area and total dendritic

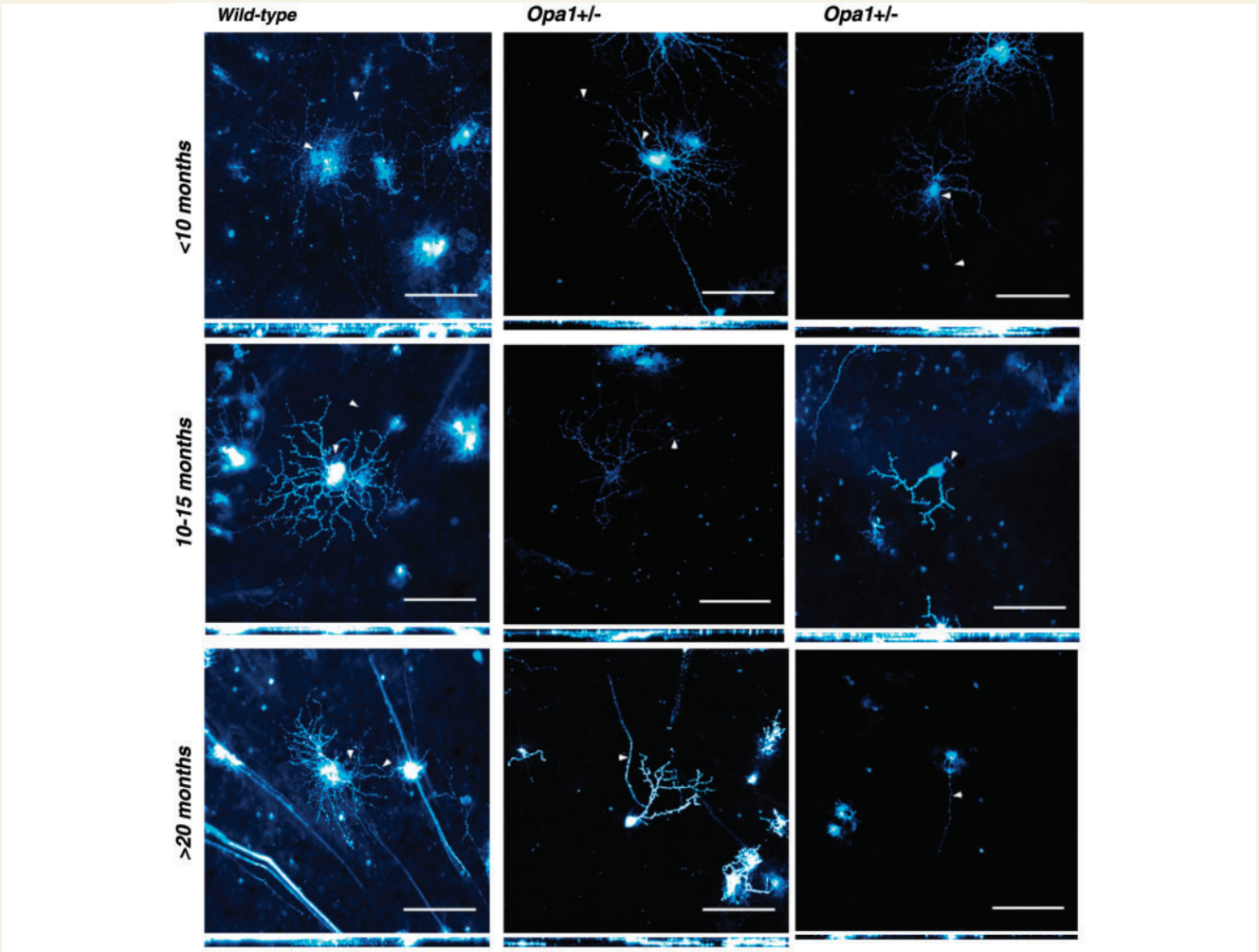

Figure 1 Compressed confocal stacks of DiOlistically labelled wild-type and *Opa1*$^{+/-}$ on-centre RGCs. There is no apparent RGC dendropathy in *Opa1*$^{+/-}$ mice aged <10 months ($n = 4$) compared with their wild-type controls ($n = 4$). There is significant on-centre RGC dendropathy in both the 10- to 15-month-old *Opa1*$^{+/-}$ mice ($n = 5$) compared with their wild-type controls ($n = 5$) and of the >20-month-old *Opa1*$^{+/-}$ mice ($n = 7$) compared with their wild-type controls ($n = 2$). Bird's-eye views (*xy* plane) (top) and side-on views (*xz* plane) (bottom) are shown for cells. Scale bar = 100 μm and is representative of both planes of view; arrow heads = axon.

length (Fig. 3) as well as unchanged dendritic complexities (AUC; $P > 0.05$).

Discussion

Here we show, for the first time, evidence of dendritic pruning in a mouse model of Opa1 dominant optic atrophy (*Opa1*^{Q285STOP} exon 8 mutation) from as early as 10 months of age. The Opa1$^{+/-}$ mouse phenotype becomes 'clinically' apparent only after 12 months and is slowly progressive with age. Visual deficits manifest as a reduction in visual acuity [measured by optokinetic drum (Davies *et al.*, 2007) and visual evoked potential changes after 10–15 months (unpublished data)]. An accompanying reduction in muscle power is apparent on rotarod testing (unpublished data), as well as wider neurological defects (Davies *et al.*, 2007). Electron microscopy on Opa1$^{+/-}$ mice reveals a loss of fibre bundle myelination in the optic nerve, as well as disrupted mitochondrial morphology, which is accompanied by increased autophagy in RGCs from 15 to 24 months of age (White *et al.*, 2009). However, there is no change in the number of axons per area of optic nerve between wild-type and *Opa1*$^{+/-}$ between 6 and 24 months of age (White *et al.*, 2009). The effects of the *Opa1*^{Q285STOP} (exon 8) mutation in our animal model appear to be more subtle than those seen in some patients with autosomal dominant optic atrophy, although the spectrum of visual deficit is very wide ranging. Nevertheless, we have evidence of dendritic atrophy at approximately the same time as changes in visual function, but preceding structural anomalies in the optic nerve that occur in the absence of axonal loss.

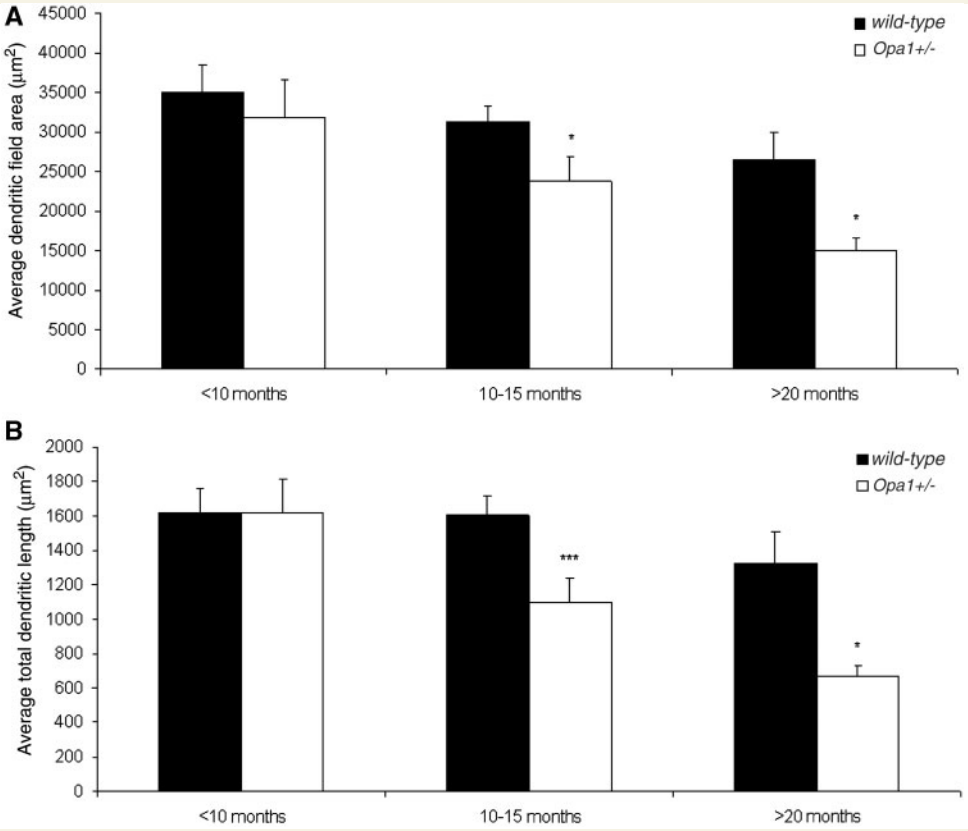

Figure 2 Opa1 deficiency leads to a reduction in dendritic field area and total dendritic length in on-centre RGCs. Average RGC dendritic field area (**A**) and average total RGC dendritic length (**B**) in the wild-type and *Opa1*$^{+/-}$ mouse. Results show a significant decrease in both the total dendritic area and average total RGC dendritic length of *Opa1*$^{+/-}$ RGCs in both the 10- to 15-month-old group (wild-type $n = 34$, *Opa1*$^{+/-}$ $n = 25$) and the >20-month-old group (wild-type $n = 5$, *Opa1*$^{+/-}$ $n = 44$) but not the <10-month-old group (wild-type $n = 21$, *Opa1*$^{+/-}$ $n = 16$). This decrease is exacerbated in the older (>20-month-old) group. *$P < 0.05$; ***$P < 0.01$; SEM = Student's *t*-test, error bars; wt = wild-type.

The process connecting changes in mitochondrial fusion with reduced visual function has been elusive (Yu-Wai-Man *et al.*, 2005). Whilst loss of RGCs by apoptosis has been proposed as the mechanism (Heiduschka *et al.*, 2009), our Opa1$^{+/-}$ mice do not show statistically significant age-dependent loss of RGCs on retinal sections and terminal deoxynucleotidyl transferase nick end labelling staining has not indicated an increase in apoptosis (unpublished data), which is consistent with this observation. By contrast, our data indicate marked changes in RGC connectivity at the onset of the development of visual defects. Studies in human patients with OPA1 autosomal dominant optic atrophy have been limited by the paucity of pathological data. RGC numbers from patients with autosomal dominant optic atrophy are lacking and broad conclusions are based on the study of two elderly patients with autosomal dominant optic atrophy with severe and advanced end-stage disease, in whom no RGC counts were undertaken (Kjer *et al.*, 1983). However, electrophysiological studies in patients are consistent with both the loss of RGCs evidenced by changes in the pattern electroretinogram P50:N95 ratio, as well as RGC dysfunction resulting in delayed visual evoked potential responses (Berninger *et al.*, 1991; Holder *et al.*, 1998). Our data from this Opa1$^{+/-}$ mouse model support the development of RGC dysfunction as an early step in the pathophysiology associated with defects in mitochondrial fusion.

We segregated the RGCs into on- and off-centre groups by their location in the inner plexiform layer (Fig. 3) and saw a dramatic difference between the two. The differential effects of the mutation on dendritic morphology in the on- and off-centre pathways is of interest, since it may shed light on the mechanisms of dendrite change in Opa$^{+/-}$ deficits. On- and off-centre pathways in the mammalian retina are partially separated in the visual pathways at the thalamic and cortical levels, with different stimulus and neurotransmitter requirements (Pourcho *et al.*, 1996; Xu *et al.*, 2007; Marc *et al.*, 2008). One explanation for this difference is that on-centre RGCs laminate in sublamina *b* of the inner plexiform layer making high energy, slow/sustained glutaminergic synapses with bipolar cells. By contrast, off-centre RGCs are restricted to sublamina *a* of the inner plexiform layer, contacting amacrine cells via GABAergic synapses as well as those glutaminergic synapses from bipolar cells. These GABAergic synapses have a lower energy demand, as they operate near the ΔEq_{Chl} and the polarized changes are small. The observed selective neuronal vulnerability may therefore reflect the higher energy demands of on-centre RGCs (Mattson and Magnus, 2006). In the Opa1$^{+/-}$ mouse, dysfunctional mitochondria in RGCs could

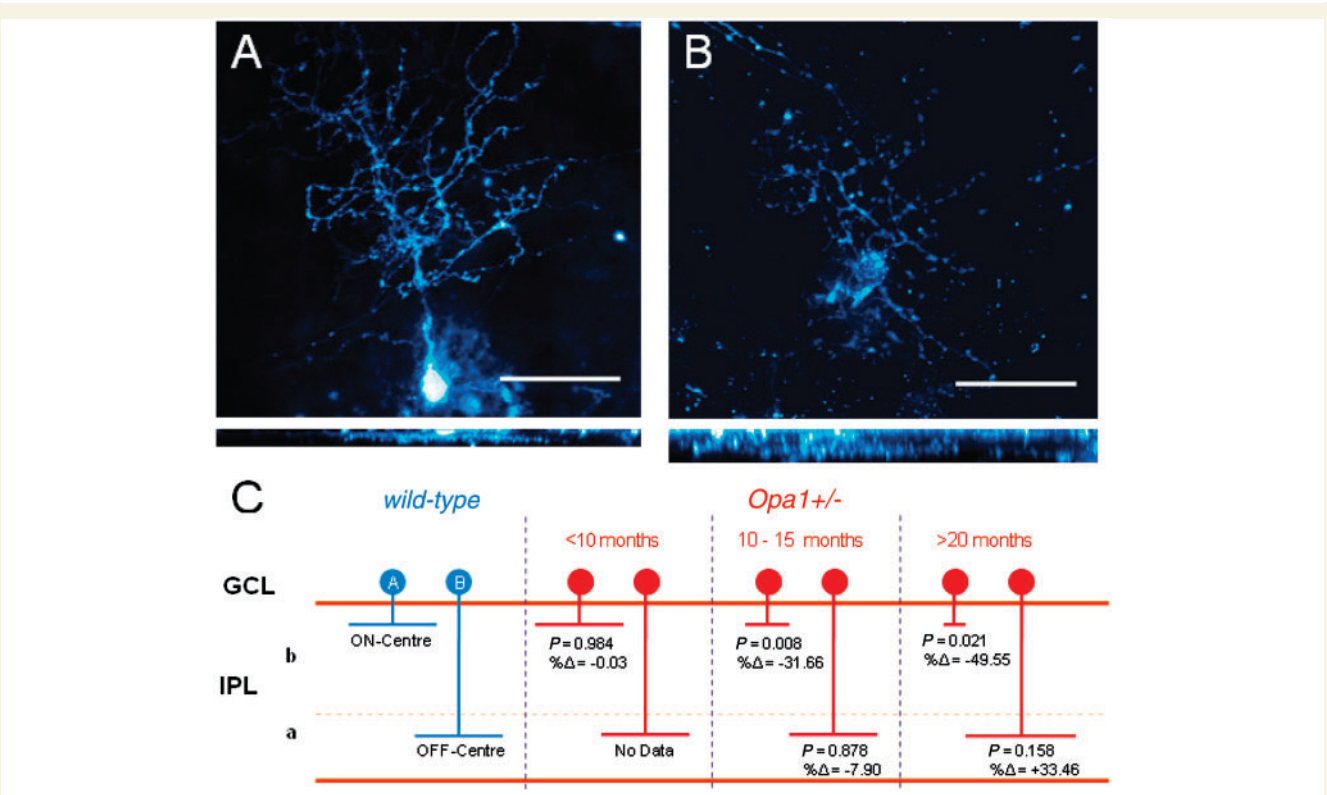

Figure 3 Opa1 deficiency leads to selective dendritic pruning of on-centre RGCs. Examples of on- (**A**) and off- (**B**) centre RGCs from an adult (10-month-old) wild-type mouse noting the different levels of dendritic ramification in the inner plexiform layer (Xu *et al.*, 2007) with the dendrites of on-centre RGCs ramifying in sublamina *b* (close to the level of the cell body) and the dendrites of off-centre RGCs ramifying in sublamina *a* (close to the inner nuclear layer). Scale bar = 25 μm. Total dendritic length is dramatically reduced in the on-centre RGCs of 10- to 15-month-old and >20-month-old mice (**C**) while remaining statistically unchanged in off-centre RGCs. *P* = Student's *t*-test, %Δ = percentage change from wild-type. GCL = ganglion cell layer; IPL = inner plexiform layer.

lead to damage by increased reactive oxygen species, lipid peroxidation leading to energy depletion (through ATPase dysfunction) and slower vesicle recycling leading to synaptic, and consequently dendritic atrophy as well as lower rates of Ca^{2+} sequestering (shown to cause neuritic degeneration). Preferential loss of on-centre RGCs has a number of implications, including the disruption of a light-sensitive pathway (though the survival of a dark-sensitive pathway), leading to visual dysfunction and ultimately loss of vision.

Analysis of mutations in patients with OPA1 autosomal dominant optic atrophy suggests two principle mechanisms by which OPA1 mutation affects mitochondrial function: (i) haploinsufficiency (nonsense mutations) and (ii) a potential dominant negative effect (missense mutations). Data from patient fibroblasts (Arnoult *et al.*, 2005; Olichon *et al.*, 2007; Amati-Bonneau *et al.*, 2008) suggest that a number of cellular effects, such as mitochondrial DNA deletions, fusion defects and reduced ATP synthesis, increase in susceptibility to apoptosis or are vulnerable to oxidative stress. We have shown by laser capture microscopy of RGCs from our $Opa1^{+/-}$ mouse model of autosomal dominant optic atrophy that no accumulation of secondary mitochondrial defects occurs and that there is no primary cyclo-oxygenase deficiency (Yu-Wai-Man *et al.*, 2009), excluding these two as likely mechanisms in our model.

Since mitochondria are significant generators of reactive oxygen species, they are particularly vulnerable to oxidative stress. Mitochondrial function may be modulated in a number of ways, including agents that may increase ATP production [idebenone (Kerr, 2010)], agents that can reduce reactive oxygen species production [co-enzyme Q (Nakajima *et al.*, 2008), minocycline (Shimazawa *et al.*, 2005), superoxide dismutase 1 (Yarosh *et al.*, 2008) and resveratrol (Kaeberlein 2010)] and those that may modulate the mitochondrial permeability transition pore and inhibit loss of mitochondria membrane potential [cyclosporine (Cook *et al.*, 2009)]. Increasing evidence from cell lines and *Drosophila* mutant (dOpa1) (Yarosh *et al.*, 2008; Tang *et al.*, 2009) have shown that *Opa1* mutation causes an increase in reactive oxygen species production and mitochondrial fragmentation (Kanazawa *et al.*, 2008), and superoxide dismutase 1 and vitamin E are able to reverse the mutant phenotype of the dOPA1. This points to the exciting potential of antioxidants as therapeutic agents for autosomal dominant optic atrophy (Levin, 2007; Kerr, 2010).

Our findings therefore reveal a potentially unique window of opportunity for the exploration of therapeutic intervention in the mouse model of autosomal dominant optic atrophy, starting at a point in the disease before significant visual and RGC loss.

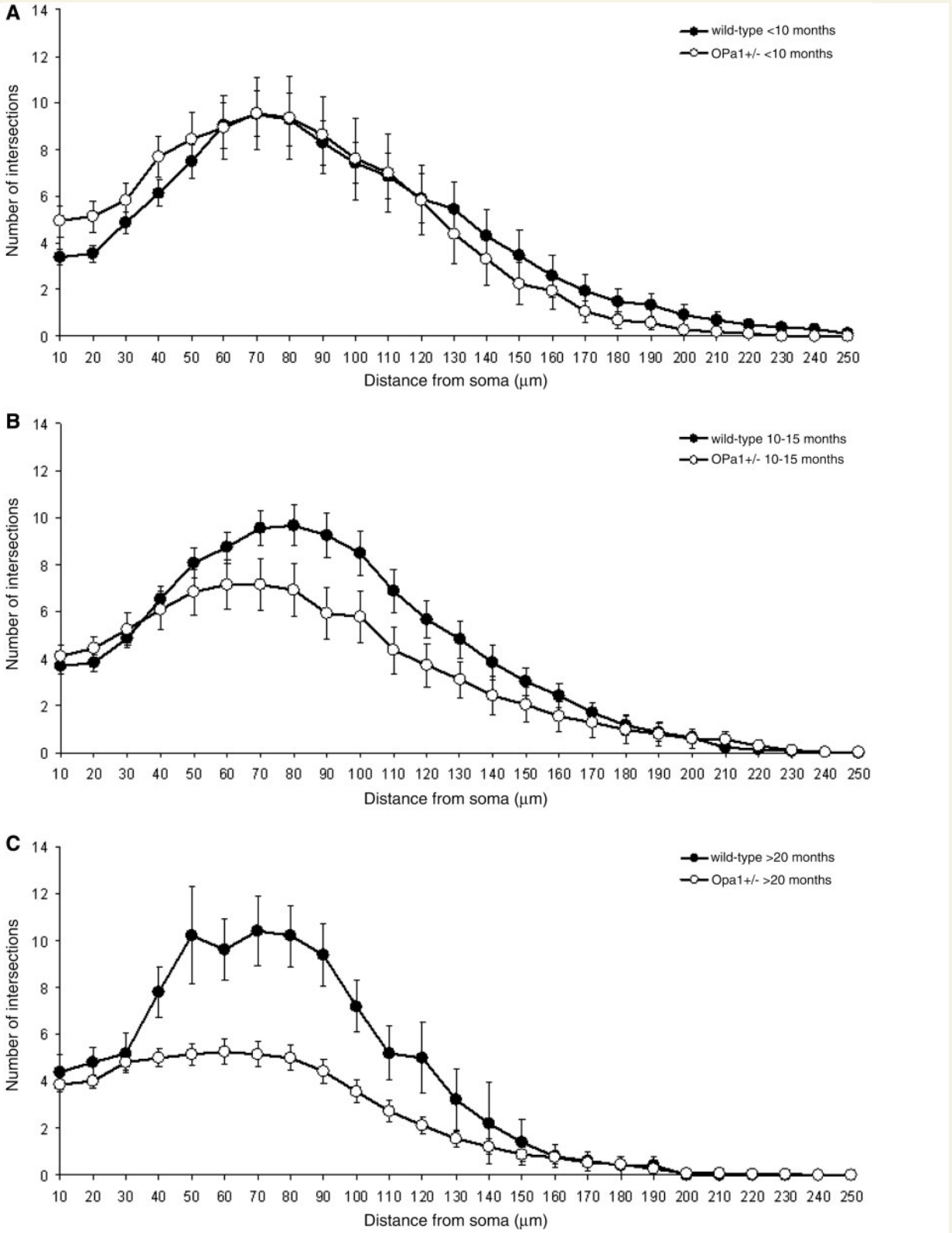

Figure 4 RGC Sholl analyses of wild type and *Opa1*$^{+/-}$ mice. Results show no difference in dendritic complexity of on-centre RGCs in the <10-month-old group (**A**) (wild-type $n = 21$, *Opa1*$^{+/-}$ $n = 16$) (AUC $P = 0.949$) but a clear difference in the 10- to 15-month-old group (**B**) (wild-type $n = 34$, *Opa1*$^{+/-}$ $n = 25$) (AUC $P = 0.137$) and a significant difference in the >20-month-old group (**C**) (wild-type $n = 5$, *Opa1*$^{+/-}$ $n = 44$) (AUC $P = 0.047$). Error bars indicate SEM; wt = wild-type.

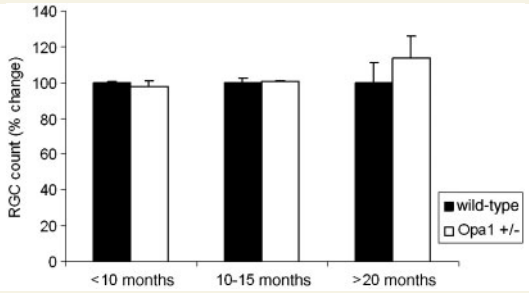

Figure 5 RGC counts in the wild type and *Opa1*$^{+/-}$ mouse as established by Hoechst stain and Haematoxylin and Eosin. Results show no significant change in RGC counts in the *Opa1*$^{+/-}$ mouse compared with wild-type across all age groups. wt = wild-type.

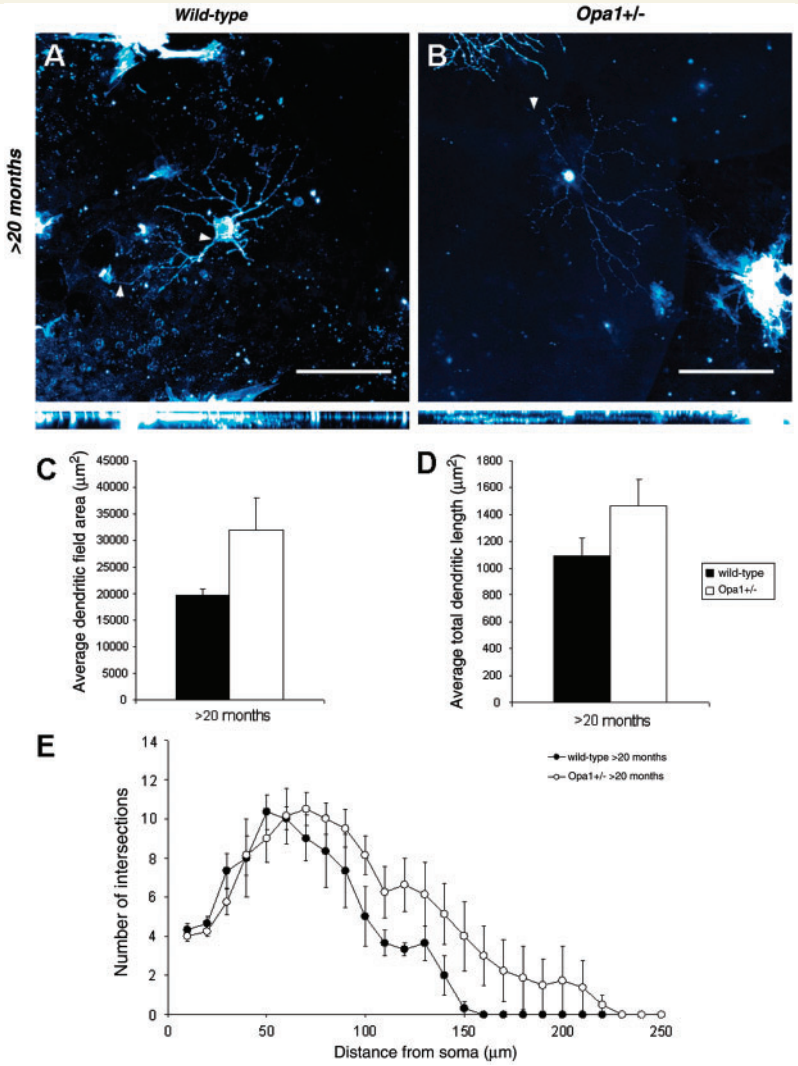

Figure 6 Opa1 deficiency has no effect on the dendritic morphology of off-centre RGCs. Where severe dendritic atrophy is present in the >20-month-old *Opa1*$^{+/-}$ on-centre RGCs, our results show no significant change in the dendritic morphologies of *Opa1*$^{+/-}$ off-centre RGCs ($n = 8$) compared with wild type ($n = 3$). Compressed confocal stacks of DiOlistically labelled wild-type (**A**) and *Opa1*$^{+/-}$ (**B**) off-centre RGCs. Bird's-eye views (*xy* plane) (top) and side-on views (*xz* plane) (bottom) are shown for cells. Scale bar = 100 μm and is representative of both planes of view; arrow heads = axon. Average RGC dendritic field area (**C**) and average total RGC dendritic length (**D**) in the wild-type and *Opa1*$^{+/-}$ mouse. Results show no significant change between wild-type and *Opa1*$^{+/-}$ mice. $P > 0.05$ for all bars; Student's *t*-test. (**E**) RGC Sholl analyses of wild-type and *Opa1*$^{+/-}$ mice. Although there is a great difference in dendritic complexity of on-centre RGCs in the *Opa1*$^{+/-}$ >20-month-old group, our results show no difference in dendritic complexity of off-centre RGCs in the >20-month-old group. Error bars indicate SEM; wt = wild-type.

Acknowledgements

We gratefully acknowledge Dr Malgorzata Piechota and Dr Vanessa Davies for RGC counts of >20-month-old mice. This work was presented in part at the Association for Research in Vision and Ophthalmology (ARVO) Annual Congress, May 2010.

Funding

Medical Research Council, UK.

References

Aijaz S, Erskine L, Jeffery G, Bhattacharya SS, Votruba M. Developmental expression profile of the optic atrophy gene product: OPA1 is not localized exclusively in the mammalian retinal ganglion cell layer. Invest Ophthalmol Vis Sci 2004; 45: 1667–73.

Alavi MV, Bette S, Schimpf S, Schuettauf F, Schraermeye U, Wehrl HF, et al. A splice site mutation in the murine Opa1 gene features pathology of autosomal dominant optic atrophy. Brain 2007; 130: 1029–42.

Alexander C, Votruba M, Pesch UE, Thiselton DL, Mayer S, Moore A, et al. OPA1, encoding a dynamin-related GTPase, is mutated in autosomal dominant optic atrophy linked to chromosome 3q28. Nat Genet 2000; 26: 211–15.

Amati-Bonneau P, Valentino ML, Reynier P, Gallardo ME, Bornstein B, Boissière A, et al. OPA1 mutations induce mitochondrial DNA instability and optic atrophy 'plus' phenotypes. Brain 2008; 131: 338–51.

Arnoult D, Grodet A, Lee YJ, Estaquier J, Blackstone C. Release of OPA1 during apoptosis participates in the rapid and complete release of cytochrome *c* and subsequent mitochondrial fragmentation. J Biol Chem 2005; 280: 35742–50.

Berninger TA, Jaeger W, Krastel H. Electrophysiology and colour perimetry in dominant infantile optic atrophy. Br J Ophthalmol 1991; 75: 49–52.

Carelli V, La Morgia C, Iommarini L, Carroccia R, Mattiazzi M, Sangiorgi S, et al. Mitochondrial optic neuropathies: how two genomes may kill the same cell type? Biosci Rep 2007; 27: 173–84.

Carelli V, Ross-Cisneros FN, Sadun AA. Optic nerve degeneration and mitochondrial dysfunction: genetic and acquired optic neuropathies. Neurochem Int 2002; 40: 573–84.

Chen H, Chomyn A, Chan DC. Disruption of fusion results in mitochondrial heterogeneity and dysfunction. J Biol Chem 2005; 280: 26185–92.

Chen H, Detmer SA, Ewald AJ, Griffin EE, Fraser SE, Chan DC. Mitofusins Mfn1 and Mfn2 coordinately regulate mitochondrial fusion and are essential for embryonic development. J Cell Biol 2003; 160: 189–200.

Chen H, McCaffery JM, Chan DC. Mitochondrial fusion protects against neurodegeneration in the cerebellum. Cell 2007; 130: 548–62.

Cook AM, Whitlow J, Hatton J, Young B. Cyclosporine A for neuroprotection: establishing dosing guidelines for safe and effective use. Expert Opin Drug Saf 2009; 8: 411–19.

Davies VJ, Hollins AJ, Piechota MJ, Yip W, Davies JR, White KE, et al. Opa1 deficiency in a mouse model of autosomal dominant optic atrophy impairs mitochondrial morphology, optic nerve structure and visual function. Hum Mol Genet 2007; 1: 1307–18.

Delettre C, Lenaers G, Griffoin JM, Gigarel N, Lorenzo C, Belenguer P, et al. Nuclear gene OPA1, encoding a mitochondrial dynamin-related protein, is mutated in dominant optic atrophy. Nat Genet 2000; 26: 207–10.

Ferre M, Amati-Bonneau P, Tourmen Y, Malthiery Y, Reynier P. eOPA1: an online database for OPA1 mutations. Hum Mutat 2005; 25: 423–8.

Gan WB, Grutzendler J, Wong WT, Wong RO, Lichtman JW. Multicolor "diolistic" labeling of the nervous system using lipophilic dye combinations. Neuron 2000; 27: 219–25.

Gutierrez H, Davies AM. A fast and accurate procedure for deriving the Sholl profile in quantitative studies of neuronal morphology. J Neurosci Methods 2007; 163: 24–30.

Heiduschka P, Schnichels S, Fuhrmann N, Hofmeister S, Schraermeyer U, Wissinger B, et al. Retinal ganglion cells are primarily affected in an animal model of OPA1 associated autosomal dominant optic atrophy. Invest Ophthalmol Vis Sci 2009. Advance Access published on October, 15, doi:10.1167/iovs.09-3606.

Holder GE, Votruba M, Carter AC, Bhattacharya SS, Fitzke FW, Moore AT. Electrophysiological findings in dominant optic atrophy (DOA) linking to the OPA1 locus on chromosome 3q 28-qter. Doc Ophthalmol 1998; 95: 217–28.

Kaeberlein M. Resveratrol and rapamycin: are they anti-aging drugs? Bioessays 2010; 32: 96–9.

Kanazawa T, Zappaterra MD, Hasegawa A, Wright AP, Newman-Smith ED, Buttle KF, et al. The C. elegans Opa1 homologue EAT-3 is essential for resistance to free radicals. PLoS Genet 2008; 4: e1000022.

Kerr DS. Treatment of mitochondrial electron transport chain disorders: a review of clinical trials over the past decade. Mol Genet Metab 2010; 99: 246–55.

Kjer P, Jensen OA, Klinken L. Histopathology of eye, optic nerve and brain in a case of dominant optic atrophy. Acta Ophthalmol (Copenh) 1983; 61: 300–12.

Levin LA. Axonal loss and neuroprotection in optic neuropathies. Can J Ophthalmol 2007; 42: 403–8.

Li Z, Okamoto K, Hayashi Y, Sheng M. The importance of dendritic mitochondria in the morphogenesis and plasticity of spines and synapses. Cell 2004; 119: 873–87.

Marc RE. Functional anatomy of the neural retina. In: Albert DM, Miller JW, Azar DT, editors. Albert & Jakobiec's principles and practice of ophthalmology. Vol. 2. Philadelphia, PA: Saunders/Elsevier; 2008. Chapter 122. p. 1–28.

Mattson MP, Magnus T. Ageing and neuronal vulnerability. Nat Rev Neurosci 2006; 7: 278–94.

Nakajima Y, Inokuchi Y, Nishi M, Shimazawa M, Otsubo K, Hara H. Coenzyme Q protects retinal cell s against oxidative stress in vitro and in vivo. Brain Res 2008; 1226: 226–33.

Olichon A, Landes T, Arnauné-Pelloquin L, Emorine LJ, Mils V, Guichet A, et al. Effects of OPA1 mutations on mitochondrial morphology and apoptosis: relevance to ADOA pathogenesis. J Cell Physiol 2007; 211: 423–30.

Palau F, Estela A, Pla-Martín D, Sánchez-Piris M. The role of mitochondrial network dynamics in the pathogenesis of Charcot-Marie-Tooth disease. Adv Exp Med Biol 2009; 52: 129–37.

Pignatelli V, Strettoi E. Bipolar cells of the mouse retina: a gene gun, morphological study. J Comp Neurol 2004; 476: 254–66.

Pourcho RG. Neurotransmitters in the retina. Curr Eye Res 1996; 15: 797–803.

Shimazawa M, Yamashimab T, Agarwalc N, Hara H. Neuroprotective effects of minocycline against in vitro and in vivo retinal ganglion cell damage. Brain Res 2005; 1053: 185–94.

Sholl DA. Dendritic organization in the neurons of the visual and motor cortices of the cat. J Anat 1953; 97: 387–406.

Sun W, Li N, He S. Large-scale morphological survey of mouse retinal ganglion cells. J Comp Neurol 2002; 451: 115–26.

Tang S, Le PK, Tse S, Wallace DC, Huang T. Heterozygous mutation of Opa1 in Drosophila shortens lifespan mediated through increased reactive oxygen species production. PLoS One 2009; 4: e4492.

Tatsuta T, Langer T. Quality control of mitochondria: protection against neurodegeneration and ageing. EMBO J 2008; 27: 306–14.

Twig G, Elorza A, Molina AJ, Mohamed H, Wikstrom JD, Walzer G, et al. Fission and selective fusion govern mitochondrial segregation and elimination by autophagy. EMBO J 2008; 27: 433–46.

Votruba M, Fitzke FW, Holder GE, Carter A, Bhattacharya SS, Moore AT. Clinical features in affected individuals from 21 pedigrees with dominant optic atrophy. Arch Ophthalmol 1998; 116: 351–8.

Waterham HR, Koster J, van Roermund CW, Mooyer PAW, Wanders RJA, Leonard JV. A lethal defect of mitochondrial and peroxisomal fission. N Engl J Med 2007; 356: 1736–41.

White KE, Davies VJ, Hogan VE, Piechota MJ, Nichols PP, Turnbull DM, et al. OPA1 deficiency associated with increased autophagy in retinal ganglion cells in a murine model of dominant optic atrophy. Invest Ophthalmol Vis Sci 2009; 50: 2567–71.

Xu HP, Tian N. Retinal ganglion cell dendrites undergo a visual activity-dependent redistribution after eye opening. J Comp Neurol 2007; 503: 244–59.

Yarosh W, Monserrate J, Tong JJ, Tse S, Le PK, Nguyen K, et al. The molecular mechanisms of OPA1-mediated optic atrophy in Drosophila model and prospects for antioxidant treatment. PLoS Genet 2008; 4: e6.

Yu-Wai-Man CY, Chinnery PF, Griffiths PG. Optic neuropathies – importance of spatial distribution of mitochondria as well as function. Med Hypotheses 2005; 65: 1038–42.

Yu-Wai-Man P, Davies VJ, Piechota MJ, Cree LM, Votruba M, Chinnery PF. Secondary mtDNA defects do not cause optic nerve dysfunction in a mouse model of dominant optic atrophy. Invest Ophthalmol Vis Sci 2009; 14: 4561–6.